

Inhibition of ion diffusion/migration in perovskite p-n homojunction by polyetheramine insert layer to enhance stability of perovskite solar cells with p-n homojunction structure

Dong Wei^{1#*}, Qingrui Cai^{1#}, Shidong Cai¹, Yongjing Wu¹, Mingliang Wang¹, Peng Cui^{2*}, Jun Ji^{3*}, Zhirong Zhang⁴, Luyao Yan², Jiahuang Zhang¹, Jiaqi Luo¹, Xiaodan Li⁵, Meicheng Li^{2*}

¹ College of Physics and Energy, Fujian Normal University, FuZhou, 350117, P. R. China

² School of New Energy, North China Electric Power University, Beijing, 102206, P. R. China

³ Beijing Huairou Laboratory, Beijing 101400, P. R. China

⁴ Institute of New Energy, HeXi University, Zhangye, 734000, P. R. China

⁵ Xiamen Univ. Technol., Sch. Mat. Sci. & Engn., Fujian Prov. Key Lab Funct. Mat. & Applicat., Xiamen, 361024, P. R. China

These authors contributed equally.

Correspondence: q397983012@126.com (D. Wei); cuipengmvp@163.com (P. Cui); jjun@hrl.ac.cn (J. Ji) mcli@ncepu.edu.cn (M. Li)

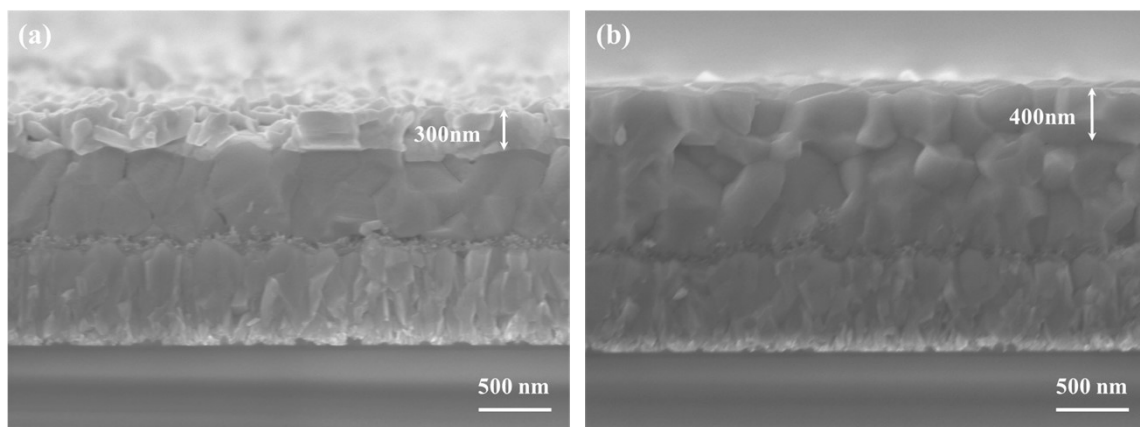


Figure S1. Cross-sectional SEM images of (a) the n-type perovskite film with PbI₂ layer and (b) p-n homojunction.

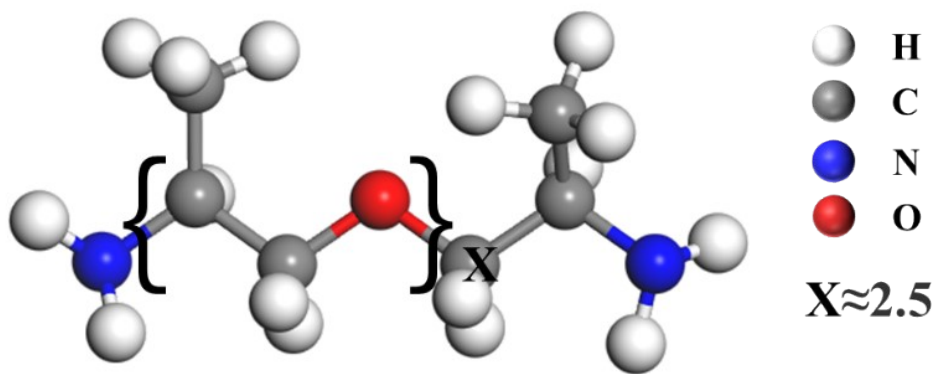


Figure S2. The molecular structure of the PEA polymer

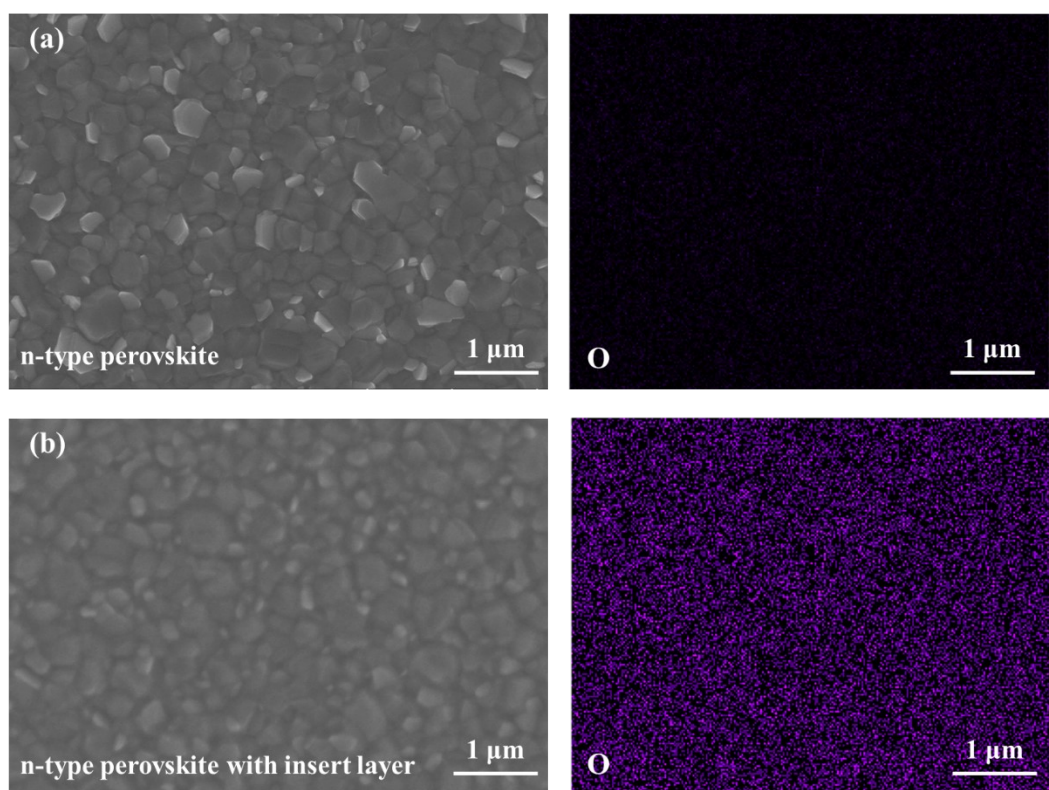


Figure S3. Top view SEM-EDS images of n-type perovskite (a) without or (b) with PEA after the annealing.

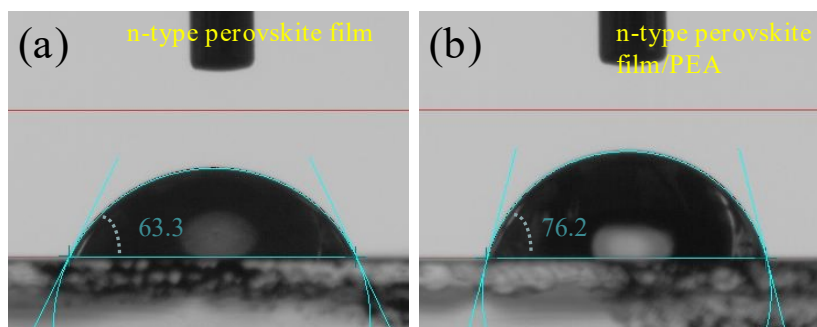


Figure S4. Contact angles of perovskite precursor solutions on (a) n-type perovskite film and (b) n-type perovskite film with PEA.

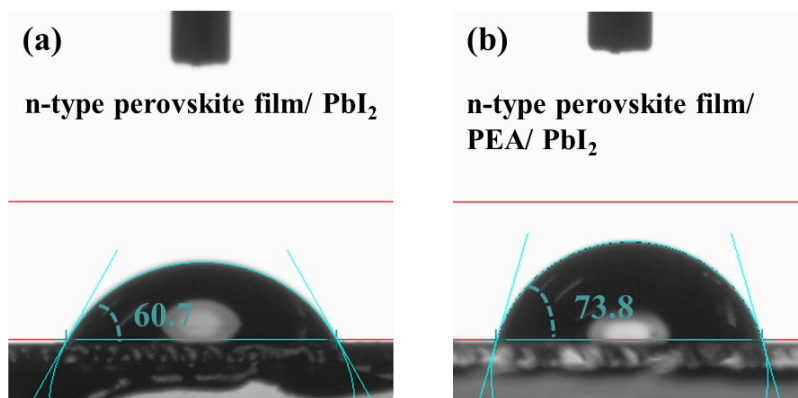


Figure S5. Contact angles of perovskite precursor solutions on (a) PbI₂ on n-type perovskite film and (b) PbI₂ on n-type perovskite film with PEA.

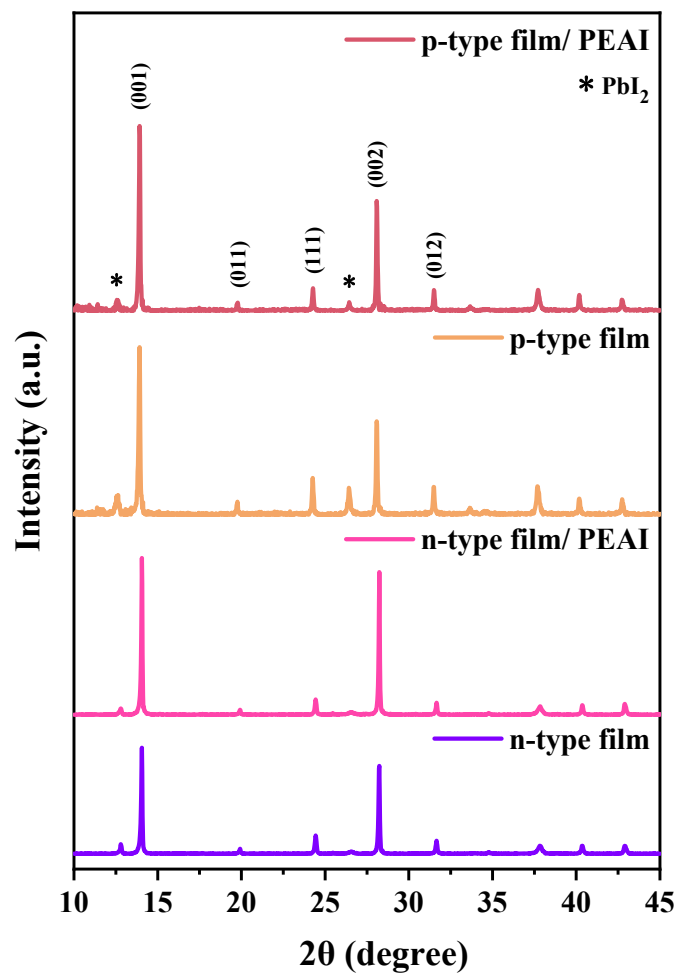


Figure S6. XRD patterns of n-type perovskite film, n-type perovskite film with and without the PEAI and p-type perovskite film with and without the PEAI

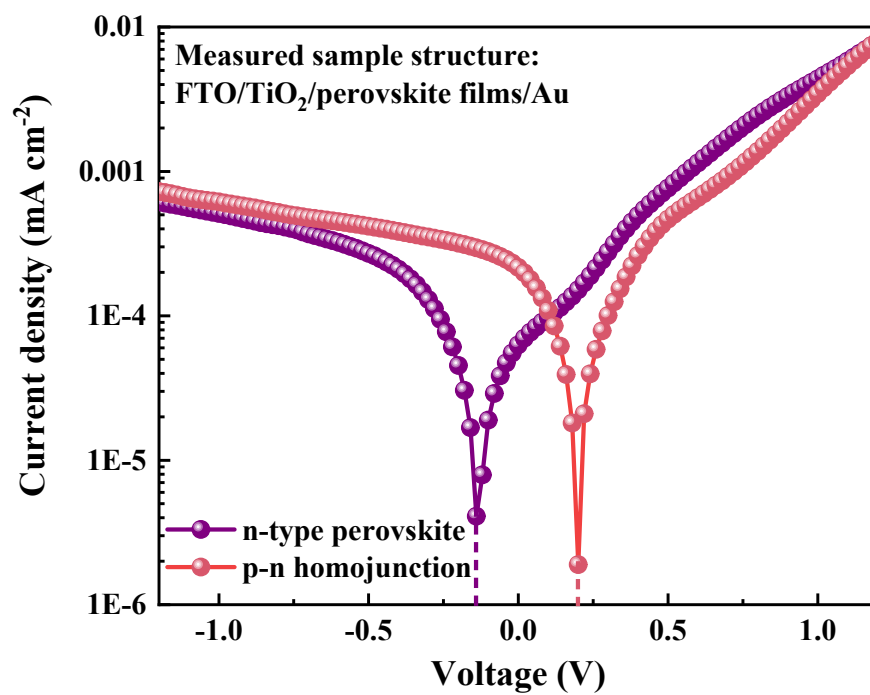


Figure S7. Dark J-V curves of the n-type perovskite film and the p-n homojunction.

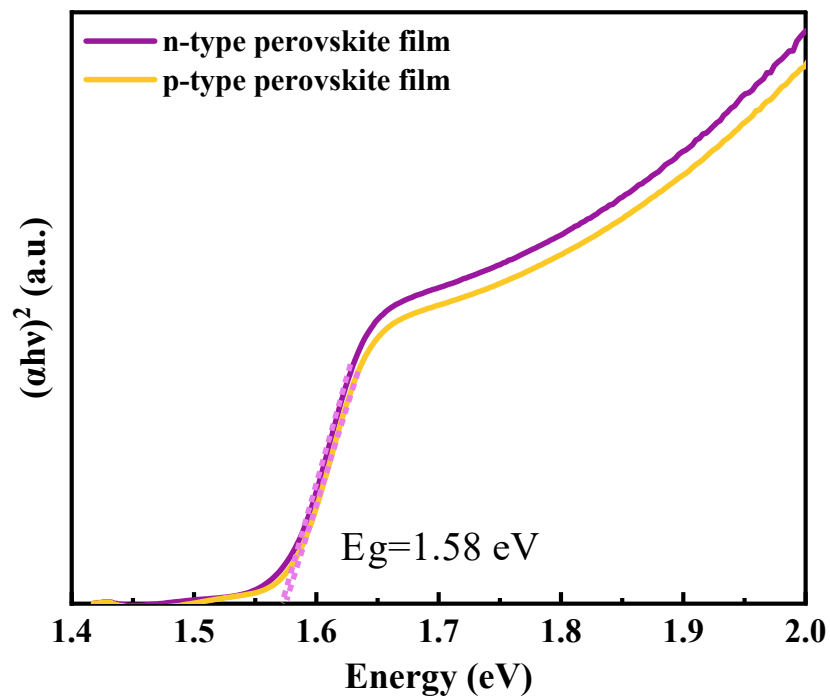


Figure S8. Tauc plots of n-type and p-type perovskite films.

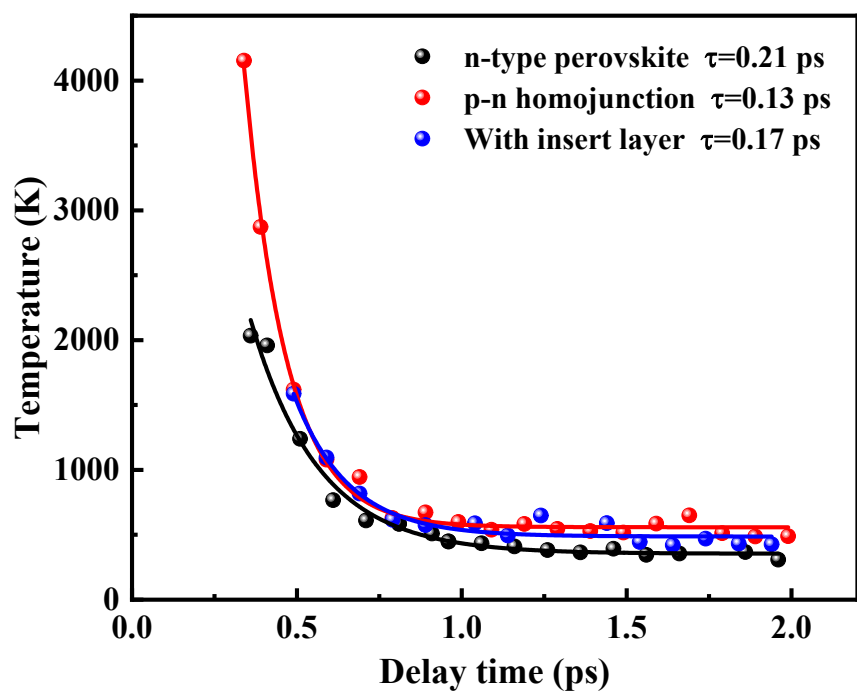


Figure S9. Hot-carrier temperature as a function of delay time for different types of perovskite films.

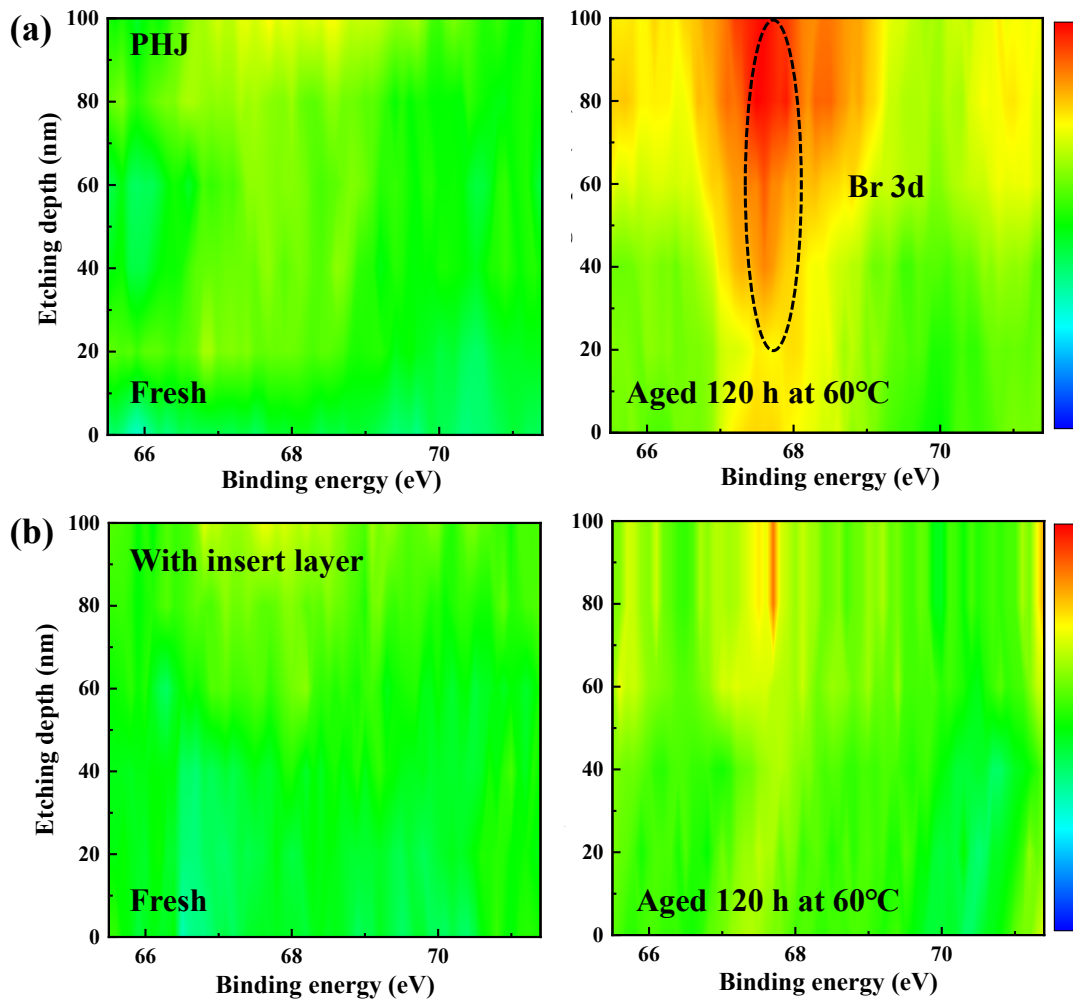


Figure S10. Evolution of Br 3d peaks (obtained from XPS depth profiling) of the PHJ (a) without and (b) with insert layer.

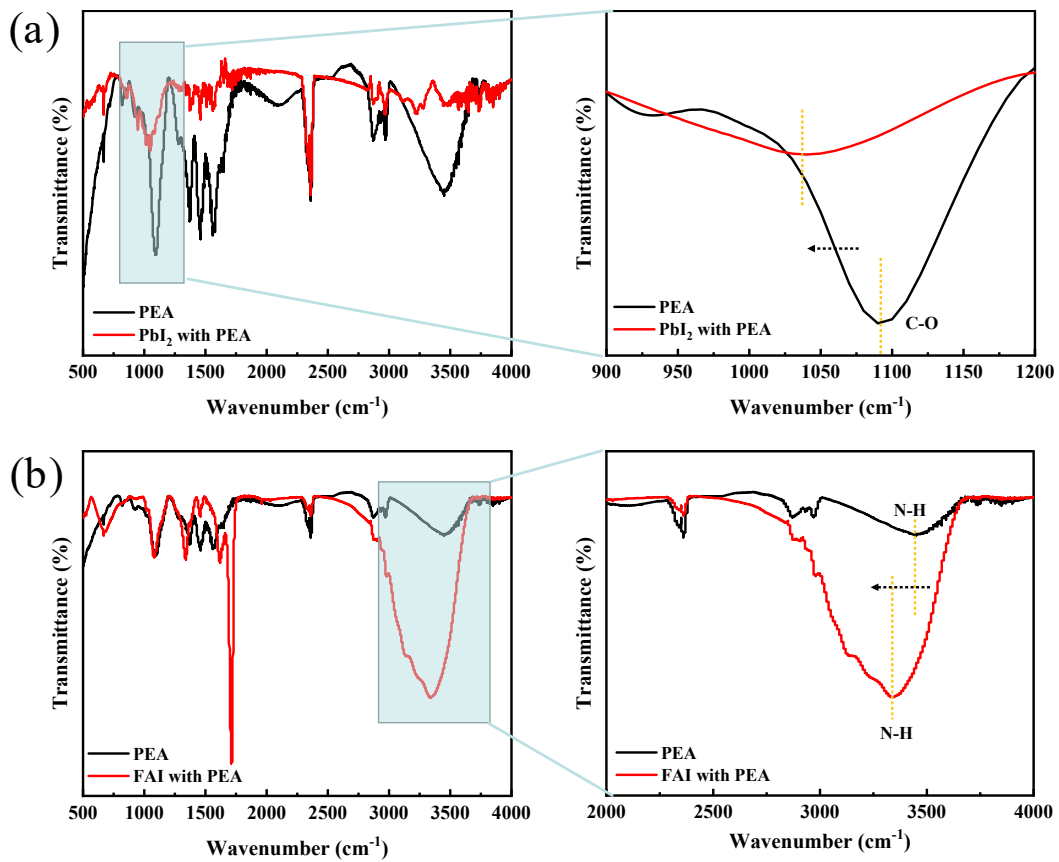


Figure S11. FTIR spectra of (a) PEA and PbI₂ with PEA samples and (b) PEA and FAI with PEA samples.

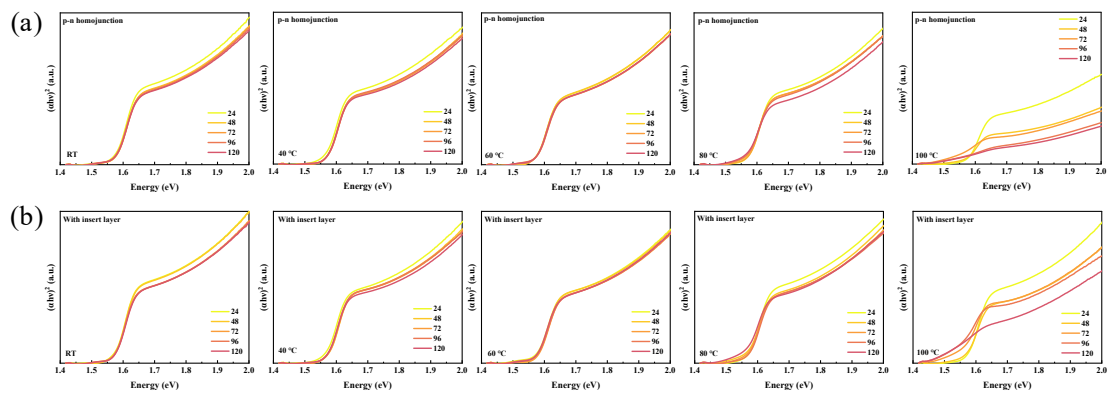


Figure S12. Evolution of Tauc plots of (a) p-n homojunction samples and (b) p-n homojunction with insert layer obtained at various temperature.

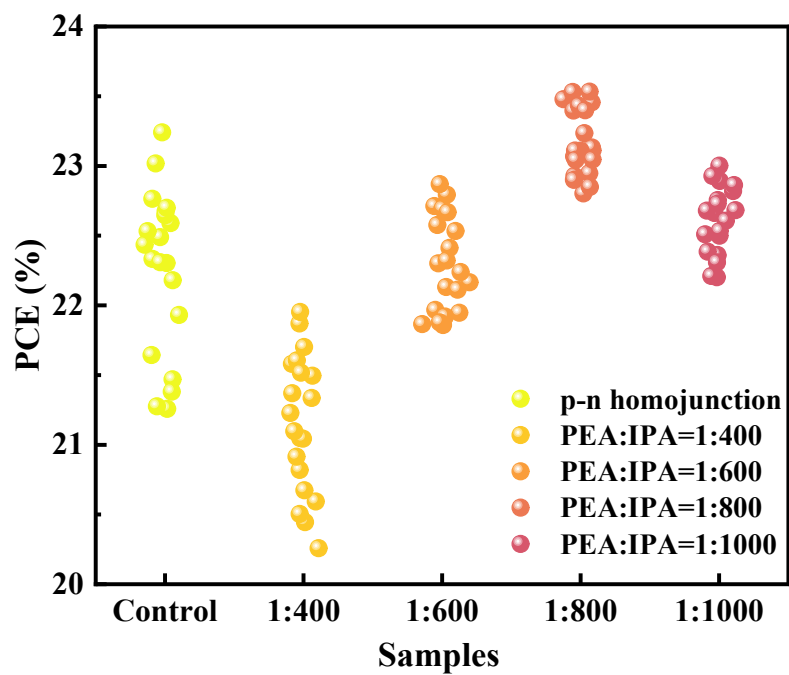


Figure S13. Statistical distributions of the PCE values of PHJ-PSCs with various thickness of insert layer. The thickness of the insert layer is controlled by the dilution ratio of the solution.

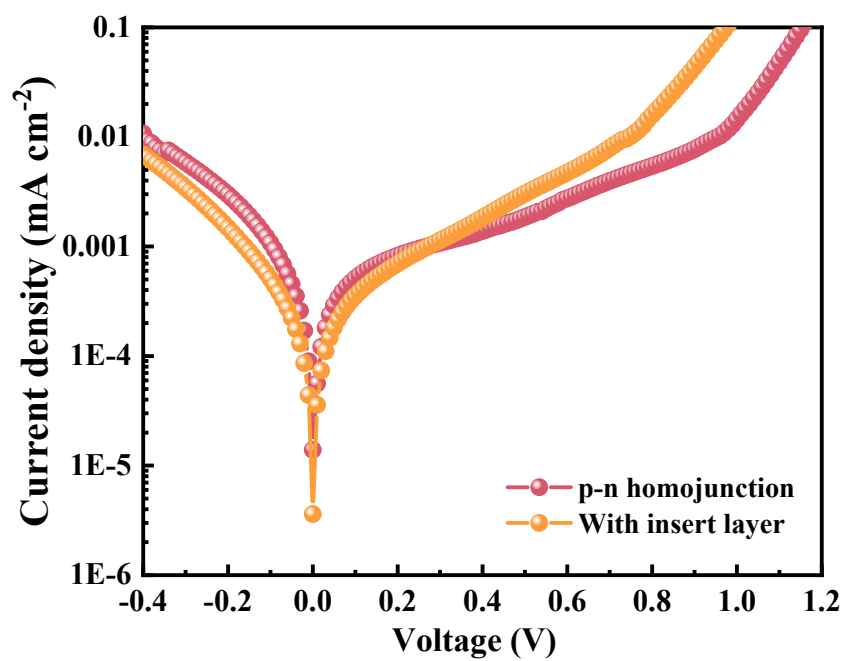


Figure S14. Dark J - V curves of the PHJ-PSCs without and with insert layer.

Table S1. The TRPL fitting parameters of different perovskite samples.

Sample	τ_1 (ns)	A_1 (%)	τ_2 (ns)	A_2 (%)	τ_{ave} (ns)
n-type perovskite	38.11	1.28	811.24	73.39	810.60
p-n homojunction	30.24	82.78	227.97	14.41	142.45
With insert layer	40.63	75.97	278.03	7.95	139.69